Journal of Peptide Science
J. Peptide Sci. 2006; **12**: 92–105
Published online 13 June 2005 in Wiley InterScience (www.interscience.wiley.com). DOI: 10.1002/psc.692

JOURNAL OF PEPTIDE SCIENCE

A theoretical study of pentacyclo-undecane cage peptides of the type (Ac-X-Y-NHMe)

KRISHNA BISETTY,[a]* FRANCESC J. CORCHO,[b] JOSEP CANTO,[b] HENDRIK G. KRUGER[c] and JUAN J. PEREZ[b]

[a] Department of Chemistry, Durban Institute of Technology, P.O. Box 1334, Durban, 4000, South Africa
[b] Department d'Enginyeria Química, UPC.ETS d'Enginyers Industrials.Av.Diagonal, 647, 08 028 Barcelona, Spain
[c] School of Chemistry, University of KwaZulu-Natal, Durban, 4041, South Africa

Received 25 February 2005; Accepted 4 May 2005

Abstract: The conformational preferences of peptides of the type, Ac-X-Y-NHMe, where X and Y = Ala, cage and Pro, were studied by means of computational techniques within the framework of a molecular mechanics approach. For each of the eight peptide analogues, extensive conformational searches were carried out using molecular dynamics (MD) and simulated annealing (SA) protocols in an iterative fashion. Both results are in good agreement and complement each other. The conformational search indicates that the cage residue restricts the conformational freedom of the dipeptide considerably in comparison with the other model residues used. This study revealed that proline exhibits a greater tendency in promoting reverse-turn characteristics in comparison to the cage peptides, which show promising β-turn characteristics. It was also found that 300–500 K is not sufficient to overcome rotational barriers for cage peptides. In all cases, the low-energy conformers have a tendency to form bent structures.

Keywords: non-natural amino acids; PCU cage dipeptide; conformational study; AMBER; simulated annealing; molecular dynamics

INTRODUCTION

The incorporation of 1-amino-adamantane (**1**) into peptides has been shown to induce a range of positive effects on the pharmacokinetic properties of drugs [1]. After Davies and co-workers [2] discovered that amantadine (**1**) exhibits antiviral properties, considerable synthetic research has taken place in the field of polycyclic compounds [3–6].

The potential therapeutic value of novel pentacyclic 'cage' compounds (Figure 1) was recently demonstrated in a number of case studies [7–10] and their activities compared favorably [11–13] with that of amantadine. The continuous advancement of experimental techniques to incorporate unnatural amino acids into proteins is steadily increasing our knowledge of biochemical systems and processes [14,15]. These efforts have led to the design of molecules as potentially useful medicinal agents [14–16].

The incorporation of cage frameworks into drugs should also have the added advantage that metabolic degradation is retarded by the inherent steric bulk of the cage skeleton, thus prolonging the activity and reducing the frequency of drug administration to the patient [1]. The rigid cage structure in some cases also induces receptor site specificity in areas such as antibacterial activity, anabolic action and analgesic activity [17–19].

It is expected that the pentacyclo-undecane (PCU) cage residue (**2**) [20] will impose large conformational constraints due to its highly bulky structure, so that peptides containing the residue will exhibit little flexibility.

Furthermore, the lypophilic nature of the cage will provide an improved pharmacokinetic profile to the peptides by enhancing drug and ion transport across cellular membranes [1,6,10,17]. In addition, it was also demonstrated that these cage amines have promising ability to deliver drugs to the central nervous system (CNS) and to cross the blood–brain barrier (BBB) [10]. The PCU cage skeleton (**2**) offers an additional interesting dimension to the series of non-natural amino acids, since it resembles an α-amino acid attached to a perfect rigid cyclohexane boat structure, as demonstrated in the alternative drawing (Figure 1). The axial hydrogen atom of the nearby CH_2 should have a pronounced influence on groups attached to the amino function.

As part of a wider research project aimed at achieving a better understanding of the conformational features of the (R)-8-amino-pentacyclo[5.4.0.0^{2,6}.0^{3,10}.0^{5,9}] undecane-8-carboxylic (PCU amino acid (**2**) [20]), an extensive conformational search was undertaken of the cage monopeptide (**3**) (Figure 2) [21].

Bisetty *et. al.* [21] revealed the presence of four low-energy conformers, C_{7ax}, C_{7eq}, 3_{10} and α_L located on the conformational space of the PCU cage residue (**3**), at both the AMBER and the *ab initio* levels. Although results from the AMBER force field favor the C_{7eq} structure in comparison with the C_{7ax} structure, which

*Correspondence to: K. Bisetty, Department of Chemistry, Durban Institute of Technology, P.O. Box 1334, Durban, 4000, South Africa; e-mail: bisettyk@dit.ac.za

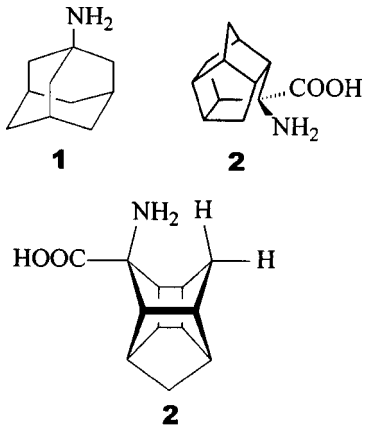

Figure 1 Amantadine (**1**) and a PCU cage amino acid (**2**). The structure of (**2**) was redrawn to emphasize the rigid cyclohexane boat structure of the PCU skeleton.

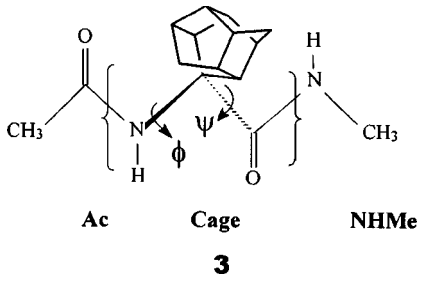

Figure 2 PCU cage monopeptide.

is favored at the *ab initio* level, the difference in relative energy is small, about 1 kcal mol^{-1}. It should also be recognized that the order of the *ab initio* result in some cases is reversed with respect to the MP2 and AMBER results [22,23].

In order to gain greater insight into the conformational flexibility of longer chains of the cage peptide, the effect of the PCU cage amino acid (**2**) on the conformational profile of a dipeptide was investigated at the AMBER force field using two alternative methodologies, viz. iterative simulated annealing (SA) [24–28] and single molecular dynamics (MD) [28–31]. The different peptidic environments chosen were: [A] = Ac-Ala-Ala-NHMe; [B] = Ac-cage-cage-NHMe; [C] = Ac-Ala-cage-NHMe; [D] = Ac-cage-Ala-NHMe; [E] = Ac-Pro-Ala-NHMe; [F] = Ac-Ala-Pro-NHMe; [G] = Ac-Pro-cage-NHMe and [H] = Ac-cage-Pro-NHMe. This series of dipeptides will allow one to investigate the conformational restrictions induced by the cage in comparison with that of Pro. As Pro is known to promote reverse-turn characteristics [32–34] it will serve as a benchmark for possible reverse-turn effects by the cage amino acid. Thus the low-energy conformers were grouped into classes of different β-turn types. The normal three parameters that define β turns [34] were used to classify the different conformers.

METHODS

All calculations were carried out within the framework of molecular mechanics, using the all-atom AMBER 5.0 force field [35]. The cage peptide was built using the PREP module of AMBER from the force field parameters described before [21].

(i) Simulated Annealing (SA)

In all cases, starting structures were prepared in an extended C_5 conformation and all calculations performed in the 'gas phase'. The initial structure was energy minimized using the conjugate gradient algorithm with the gradient convergence criteria set to 0.001 kcal mol^{-1}Å^{-1}. Subsequently, the structure was heated up to 900 K at a rate of 100 K ps^{-1}. Heating is fast in order to enable the molecule to cross the potential barriers of the different regions of the conformational space. At this point, the structure was slowly cooled down to 200 K at a rate of 7 K ps^{-1}. The structure was then minimized and saved. The same structure was used as a starting conformation for the next cycle of SA, thereby accumulating a library of 3000 structures for each of the peptide sequences, [A]–[H]. These structures were rank-ordered by energy for every 100 cycles and checked for uniqueness. A conformation was considered unique if at least one of the backbone dihedral angles was different by 60° with respect to the rest of unique conformations already on the list at the checked moment. The efficiency of this process was monitored according to the Eqn (1) shown below [25,26,28]:

$$\lambda(N) = \frac{\xi(N)100}{N\xi(100)} \quad (1)$$

The efficiency parameter, λ is computed for every 100 cycles of SA. The procedure was terminated at 3000 cycles and in all cases the calculated efficiency of the process was below 10% of the starting value, $\lambda < 0.1$.

(ii) Molecular Dynamics (MD)

An extended conformation was used as the initial conformation of the system. The system was then minimized using 10 000 steps of steepest descent, followed by a subsequent minimization using the conjugate gradient algorithm until a convergence of the gradient norm was lower than 0.001 kcal mol^{-1} Å^{-1}. The molecule was placed into a rectangular box of 30 × 25 × 20 Å3 within TIP3P water molecules [36]. The next minimization of this new system was completed when the convergence criteria was fulfilled, (0.001 kcal mol^{-1} Å^{-1}), with a cut-off of 8 Å used to evaluate non-bonded interactions, and the dielectric constant set to 1 r (distance dependence). Thereafter periodic boundary conditions were introduced and the structure was allowed to equilibrate for 200 ps at a temperature of 300 K, with the pressure set to 1 bar. SHAKE [35] was used on bonds involving hydrogen atoms with a time-step of 2 fs. After the first equilibration phase, the particle mesh Ewald (PME) [37] method was applied with a grid spacing of approximately 1 Å. The tolerance for evaluating the direct sum was set to 10^{-5} and a cutoff of 8 Å used to evaluate non-bonded interactions. The equilibration phase involved a single dynamic trajectory run for 1600 ps under these conditions. The module CARNAL [35] of AMBER 5.0 was used to calculate the backbone torsion angles.

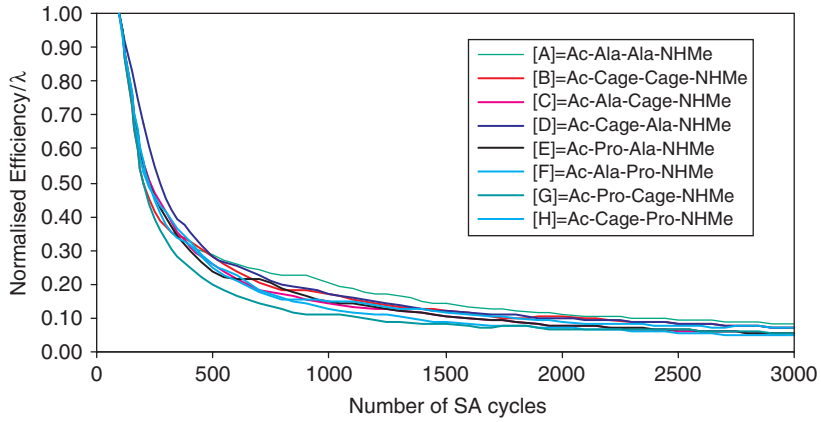

Figure 3 Normalized efficiency values for the peptide searches.

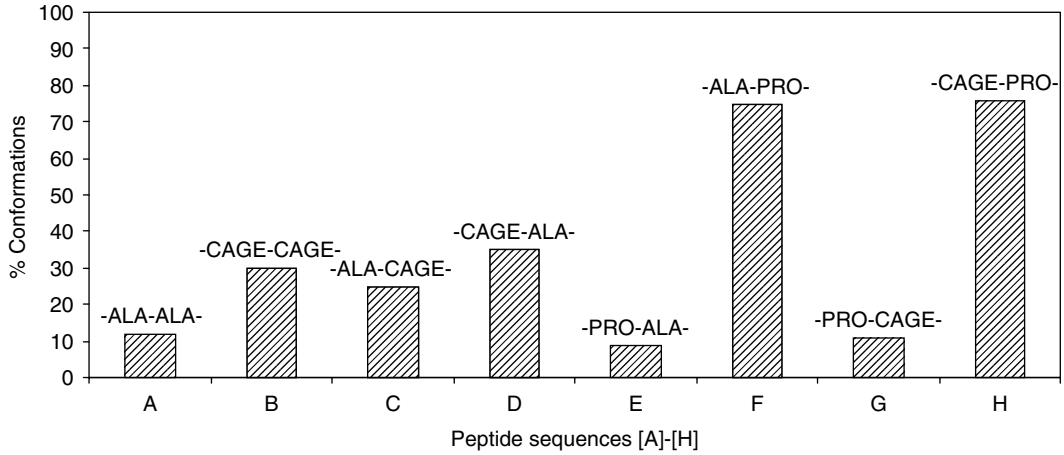

Figure 4 Percentage conformations simultaneously satisfying all three criteria for reverse-turn characteristics.

RESULTS AND DISCUSSION

(i) SA

The conformational analysis of each peptide was carried out on a subset of unique conformations within a 5 kcal mol^{-1} threshold with respect to its global minimum. In all cases, the global minimum energy was found at iteration numbers ranging from 1001 to 1023. These results suggest that the method quickly reaches low-energy conformations, and in its iterative search, the procedure is robust enough to obtain low-energy structures located in different valleys of the peptide landscape and the 3000 structures generated are sufficient for a representative SA study. For each of the peptide analogues, the evolution of the efficiency parameter, λ monitored along the conformational profile is depicted in Figure 3.

A summary of the SA results for the eight analogues exhibiting reverse-turn characteristics is presented in Table 1, and the percentage conformations that simultaneously satisfy all three criteria for reverse-turn characteristics is depicted in Figure 4. The backbone torsion angles for the library of 3000 structures corresponding to 100% of the structures sampled are presented in the Ramachandran plots shown in Figures 5[A]–[H].

Low-energy Conformations

(A) = Ac-*Ala-Ala-NHMe*. The structures of the 40 unique conformations lie in the range of energies up to 11 kcal mol^{-1} above the global minimum and 25 were within the 5-kcal mol^{-1} threshold above the global minimum energy level. On closer examination of Figure 5[A], it is evident that clustering of the backbone torsion angles occur around three regions for ϕ_1 and ϕ_2 (viz. -135°, -60° and 45°), whereas in the case of ψ_1 and ψ_2 clustering of the backbone torsion angles also occur around three similar regions (viz. 135°, -60° and -135°). The regions of the (ϕ, ψ) conformational space correspond to the two major secondary structural elements [38] viz. the α-helix $(\phi_i = -60^\circ \pm 30^\circ,\ \psi_i = -60^\circ \pm 30^\circ)_n$ and the β-pleated sheet $(\phi_i = -150^\circ \pm 30^\circ,\ \psi_i = 150^\circ \pm 30^\circ)_n$ [39]. These plots show clustering around torsion angles associated with the C_5 extended structures. It is evident from these plots (Figure 5[A]) that the global energy minimum

Table 1 Summary of percentage conformations for [A]–[H] exhibiting reverse-turn characteristics

	Percentage conformations	
	$i \rightarrow i+3$/Å	$d_{critical}$/Å
[A]	12	28
[B]	26	43
[C]	20	36
[D]	35	45
[E]	9	36
[F]	75	100
[G]	11	56
[H]	76	76

[A] = Ac-Ala-Ala-HMe
[B] = Ac-cage-cage-NHMe
[C] = Ac-Ala-cage-NHMe
[D] = Ac-cage-Ala-NHMe
[E] = Ac-Pro-Ala-NHMe
[F] = Ac-Ala-Pro-NHMe
[G] = Ac-Pro-cage-NHMe
[H] = Ac-cage-Pro-NHMe

corresponds to an extended structure ($\phi_1 = -150^\circ$, $\psi_1 = 135^\circ$ and $\phi_2 = -150^\circ$, $\psi_2 = 135^\circ$). The results are in good agreement to those obtained by Chalmers and Marshall ($\phi_1 = -162^\circ$, $\psi_1 = 140^\circ$ and $\phi_2 = -163^\circ$, $\psi_2 = 138^\circ$) [32].

(B) = Ac-*cage-cage-NHMe*. A total of 23 unique conformations were characterized ranging in energies up to 5 kcal mol^{-1} above the global minimum. The replacement of Ala by the PCU cage residue in the (i) and (i+1) positions not only restricts the conformational profile, but also causes profound changes in the appearance of the Ramachandran plots shown in Figure 5[B]. In contrast to [A] = Ac-Ala-Ala-NHMe described above, the dipeptide [B] = Ac-cage-cage-NHMe has two backbone torsion angles constrained by the introduction of the two PCU cage residues, resulting in a smaller number of unique conformations. In this case, clustering of the backbone torsion angles is similar to that associated with the α-helical structures as opposed to the extended structures indicated in [A] above. Interestingly, the result shown in the Ramachandran plots in Figure 5[B] are similar to the corresponding plots obtained in a recent study [21], where it was shown that the four low-energy structures of the cage monopeptide corresponds to the C_{7ax}, C_{7eq} α_L and 3_{10} helical conformers.

(C) = Ac-*Ala-Cage-NHMe*. The purpose of including this peptide sequence in this study was twofold. Firstly, to establish whether the extended conformations displayed by Ala as shown in [A] = Ac-Ala-Ala-NHMe are still maintained. Secondly, with the inclusion of the PCU cage residue in the second position, will the β-turn-like conformations shown in [B] = Ac-cage-cage-NHMe still be maintained for this peptide sequence? After completion of the SA procedure, 28 unique conformations were characterized ranging in energies up to 7 kcal mol^{-1} above the global minimum. Of the 28 unique conformations, 25 were in a low-energy subset within the 5-kcal mol^{-1} threshold above the global minimum. On comparing the respective portions of the Ramachandran plots of Figure 5[C] with those obtained for [A] = Ac-Ala-Ala-NHMe and [B] = Ac-cage-cage-NHMe, it was noticed that the β-turn was indeed present in this sequence as well. Closer inspection of Table 1 suggests a strong similarity in the percentages of the three criteria for reverse-turn characteristics between -cage-cage-, -Ala-cage- and -cage-Ala- (see next sequence).

(D) = Ac-*Cage-Ala-NHMe*. One would be inclined to assume that the effect of the cage in the (i) or (i+1) position is similar. Therefore, the Ramachandran plots for the cage in [C] and [D] should be approximately the same. The same is expected for Ala in the (i) and (i+1) position. The structures of the 36 unique conformations lie in the range of energies up to 9 kcal mol^{-1} above the global minimum and 30 were within the 5-kcal mol^{-1} threshold above the global minimum energy level. On closer examination of Figure 5[D] it is evident that clustering of the backbone torsion angles are similar to the corresponding backbone torsion angles shown in Figure 5[C]. In contrast to -Ala-cage-, it is observed from Figure 4 and Table 1, that -cage-Ala- is about 10% more efficient at inducing reverse-turn characteristics.

(E) = Ac-*Pro-Ala-NHMe*. In contrast to the peptide sequences [A]–[D], only 16 conformations were characterized as unique. This means that the inclusion of Pro in this peptide sequence restricts the conformational space much more severely than Ala and the PCU cage residues. Their energies ranged up to 6 kcal mol^{-1} above the global minimum; 11 of them within the 5-kcal mol^{-1} threshold above the global minimum. The plots of the backbone torsion angles are depicted by the Ramachandran plots shown in Figure 5[E]. In contrast to [A] described above, this dipeptide has its backbone torsion angles constrained by the introduction of Pro in the (i) position. This fact is clearly illustrated on closer examination of the Ramachandran plots shown in Figure 5[E]. Here, the backbone torsion angle, ϕ_1, is restricted to near -65° during the simulation, which is expected for the Pro residue, [40] while the ψ_1 torsion angle is restricted to near 135° and -45°. However, in the case of the low-energy conformers within the 5-kcal mol^{-1} energetic range, the backbone torsion angles corresponding to (-90°, 135°) are typical values for Pro [40]. On the other hand, with Ala in the (i+1) position there is no significant change in the Ramachandran plots shown in Figure 5[E] compared to Figure 5[A] or Figure 5[C]. The significance of this result is that the

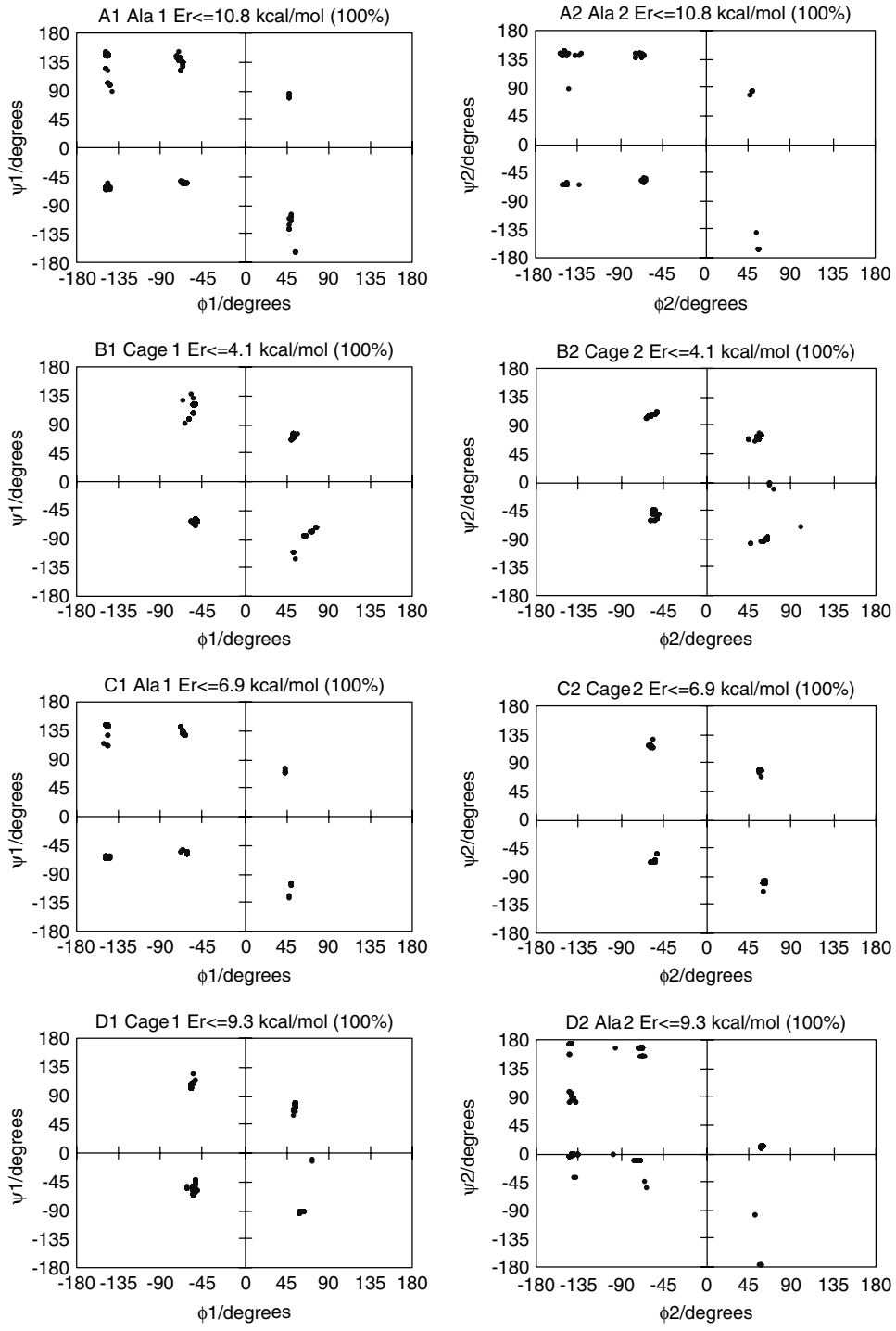

Figure 5[A]–[D] Ramachandran SA plots obtained for the peptide sequences [A]–[D].

incorporation of Pro in the (i) position causes no change in the overall conformational profile of Ala in the (i+1) position. The results presented in Table 1 suggests that Pro in the (i+1) position (see next sequence) is a much more effective β-turns promoter than Pro entering the corresponding (i) position.

(F) = Ac-*Ala-Pro-NHMe*. This sequence is required to compare the reverse-turn characteristics of Pro with that of the cage in [C] = Ac-Ala-cage-NHMe. A total of 24 unique conformations were characterized ranging in energies up to 5 kcal mol^{-1} above the global minimum. The backbone torsion angles are depicted in Figure 5[F]. On comparing Figures 5[E] with 5[F], its clear that the backbone torsion angle of Pro in the (i) position is constricted around -50°, whereas Pro in the (i+1) position is constricted around -100°, which are typical values for Pro [32–34]. Table 1 shows that

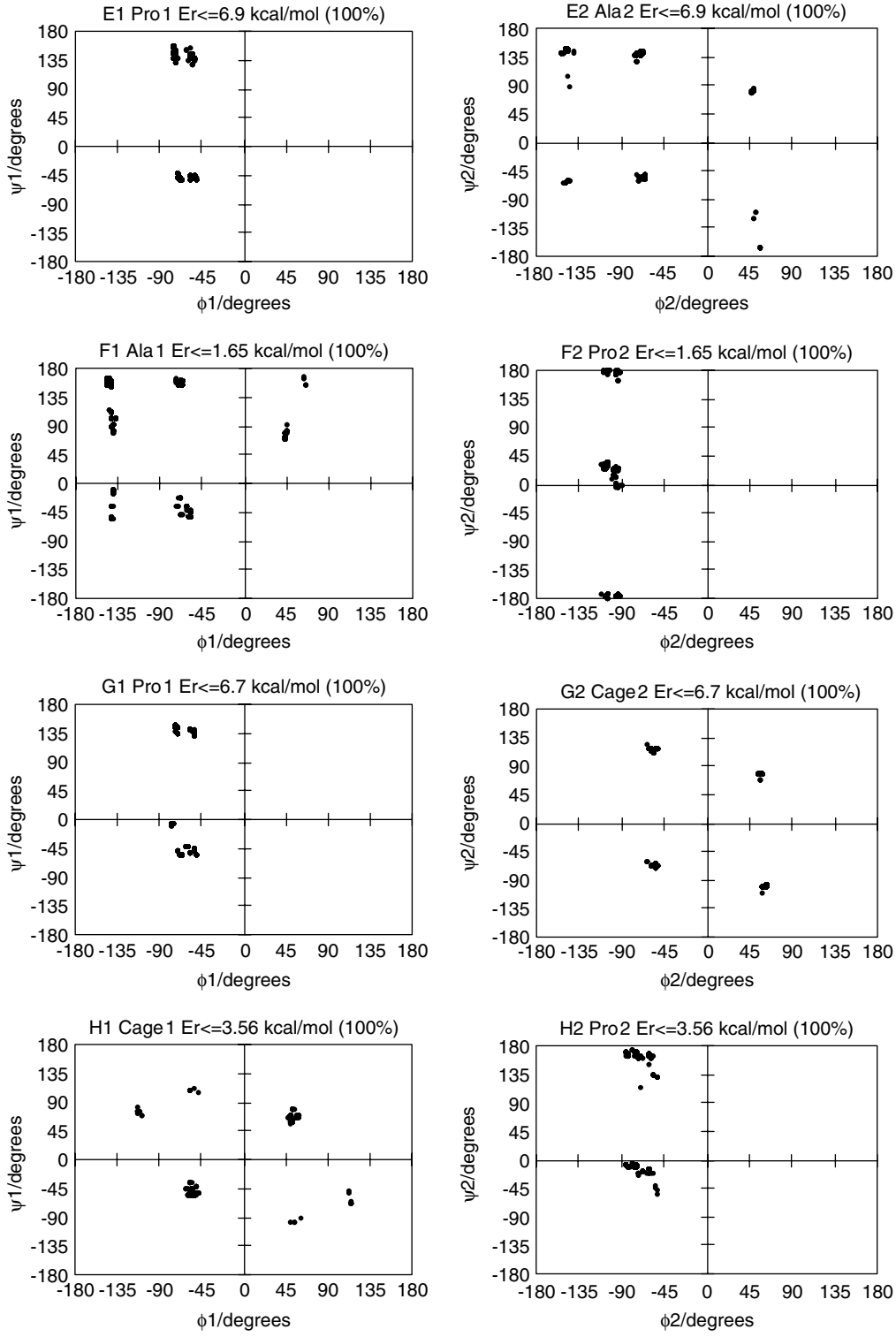

Figure 5[E]–[H] Ramachandran SA plots obtained for the peptide sequences [E]–[H].

the percentage of conformers for all three criteria for reverse-turn characteristics has risen considerably, in contrast to -Pro-Ala-. This result suggests a dramatic enhancement of the reverse-turn characteristics of Pro, similar to the results obtained by Chalmers and Marshall [32]. These results are consistent with the experimental observation that Pro is found in all four positions of β-turns in proteins, particularly in the 2nd position (i+1) [32–34].

(G) = Ac-*Pro-Cage-NHMe*. In contrast to the peptide analogues [A]–[F] described above, this dipeptide [G] has its backbone torsion angles constrained by the introduction of two cyclic residues, viz. Pro and the

PCU cage residue. In general, the incorporation of such amino acids in peptides should significantly influence the overall conformational flexibility and is an active area of research [41–43]. After 3000 cycles of SA, only 13 unique conformations were obtained, in contrast to 16 conformations obtained in [E] = Ac-Pro-Ala-NHMe. This means the greater restriction in the conformational space is attributed to the presence of the highly strained Pro and PCU cage residues. Their energies ranged up to 7 kcal mol^{-1} above the global minimum, nine of them being within the 5-kcal mol^{-1} threshold above the global minimum. To gain insight into the results of the conformational search, the plots of the backbone torsion angles are depicted by the Ramachandran plots shown in Figure 5[G]. In the case of Pro in the (i) position, the plots are similar to the plots described for Pro in the same position shown in Figure 5[E], thus confirming the tighter restriction of the (ϕ_1, ψ_1) backbone torsion angles observed for Pro [32]. On closer comparison of the Ramachandran plots of the PCU cage residue in the (i+1) position with the corresponding Ramachandran plot shown in [B] above, a tighter restriction of the (ϕ_2, ψ_2) backbone torsion angles is observed. The results in Table 1 reveal very little difference in results obtained for the percentage reverse-turn characteristics exhibited by -Pro-Ala- and -Pro-cage-. This result suggests that both Ala and cage in the (i+1) positions are poor β-turn promoters.

(H) = Ac-*Cage-Pro-NHMe*. This sequence is required to compare the reverse-turn characteristics of Pro with that of the cage in [D] = Ac-cage-Ala-NHMe. A total of 17 unique conformations were characterized ranging in energies up to 5 kcal mol^{-1} above the global minimum. The backbone torsion angles are depicted in Figure 5[H]. Interestingly, similar conformational spaces are sampled by the positions of the cage and the Pro residues in [G] and [H] respectively, as shown in Figures 5[G] and 5[H]. Table 1 shows the percentage of conformers for all three criteria for reverse-turn characteristics has risen considerably, in contrast to -Pro-cage-, resulting in a dramatic enhancement of the reverse-turn characteristics of Pro enforcing the fact that the cage is a stronger β-turn promoter in the (i) position. Interestingly, the results for the reverse-turn characteristics exhibited by the peptide sequence [F] are similar to those exhibited by the peptide sequence [H], which is consistent with the fact that Pro is most effective in inducing reverse-turn characteristics when occupied in the (i+1) position [32–34].

(ii) MD

Figure 6 shows the progression of the total energy and the temperature of a solvated molecule of [A], from the starting of the MD simulation (T = 0 K) up to 200 ps, when the temperature has stabilized to around 300 K and the system may be considered to be in equilibrium. Similar plots for the thermodynamic profiles for each of the other peptide analogues, [B]–[H] were obtained during the MD simulations. In addition to the monitoring of thermodynamic parameters over the entire MD trajectory, the second stage of the analysis involved a study of the regions accessed by each of the peptide sequences [A]–[H]. Conformations were sampled at each ps for the duration of the entire MD trajectories resulting in 1600 conformers being generated, and presented as Ramachandran plots in Figures 7[A]–[H].

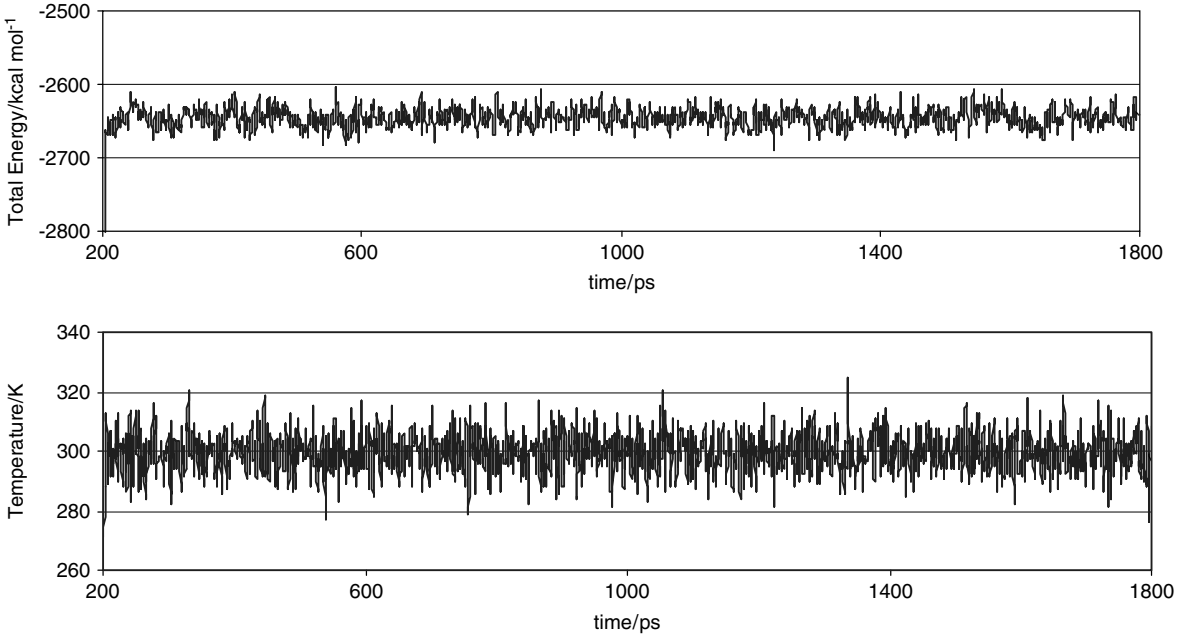

Figure 6 Observed trends in thermodynamic properties for the peptide sequences [A].

Discussion of the MD Results

(A) = Ac-*Ala-Ala-NHMe*. The Ramachandran plots A1 and A2 in Figure 7[A] correspond to the total number of conformations sampled during the 1800 ps of the MD trajectory run. On comparing this result with the corresponding SA Ramachandran plots shown in Figure 5[A], striking similarities are observed. Firstly, in both cases the first and second quadrants of the Ramachandran plots are highly populated as shown

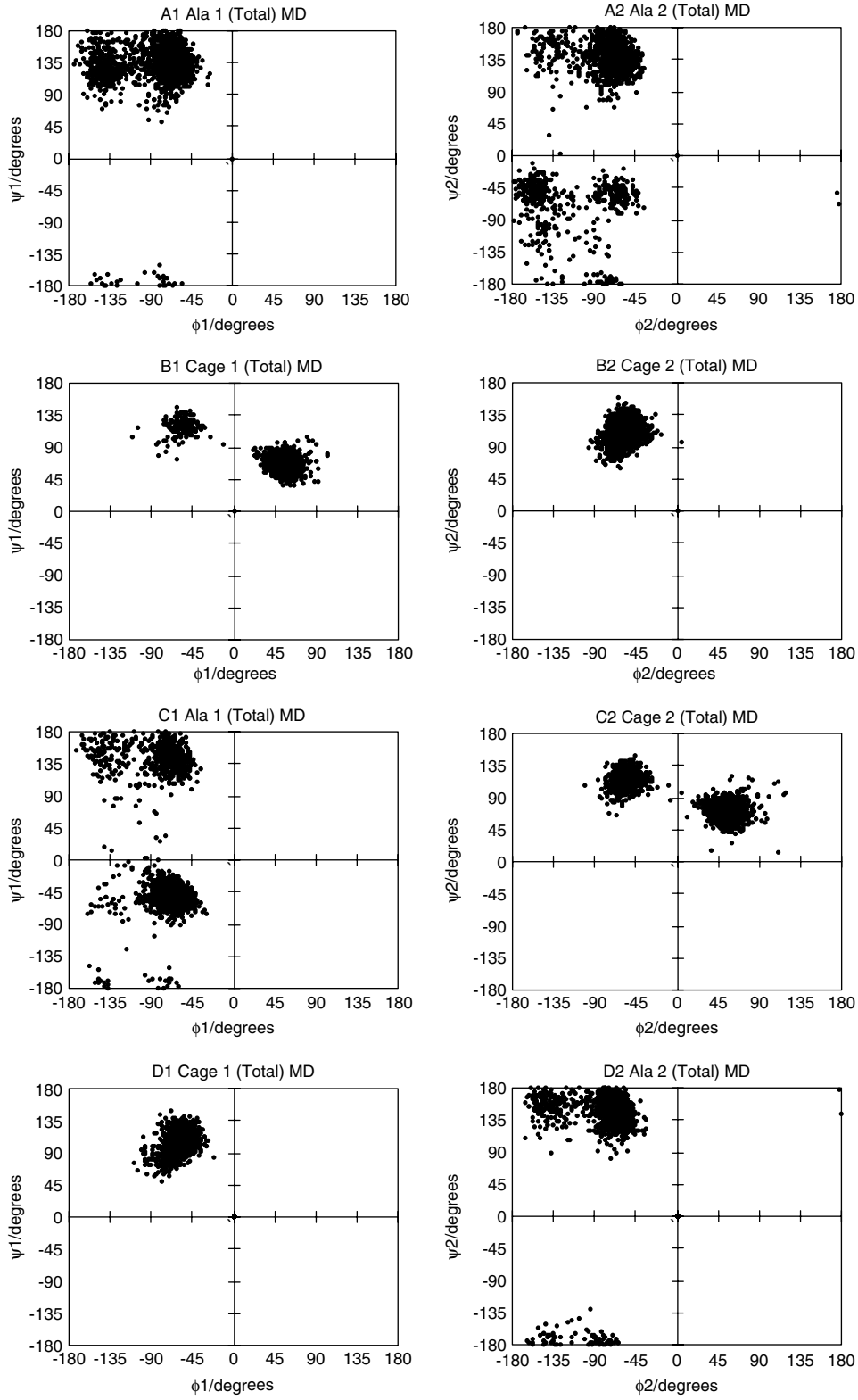

Figure 7[A]–[D] Ramachandran MD plots obtained at 300 K for the peptide sequences [A]–[D].

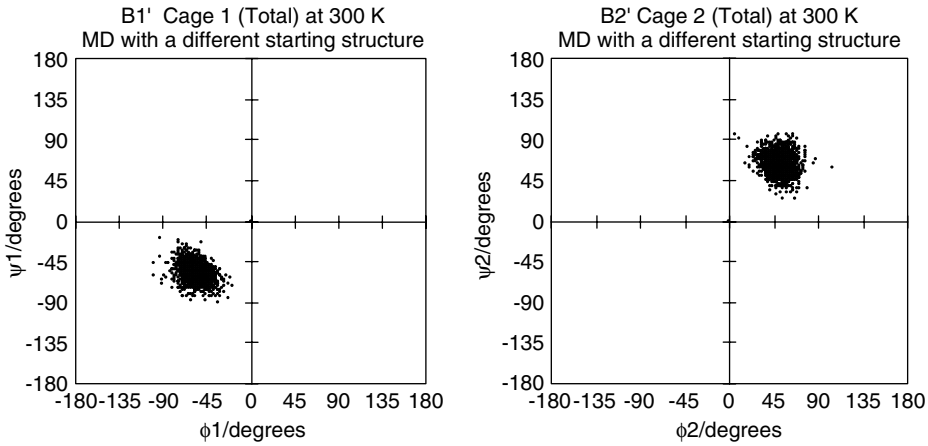

Figure 7[B'] Ramachandran MD plots obtained for a different starting structure at 300 K.

in Figure 7[A]. This indicates that the possible areas accessed for the duration of the entire MD simulation are similar to those obtained for SA in the case of [A]. Thus in both SA and MD simulations the conformers show clustering around torsion angles of $\pm 180^{\circ}$ associated with the C_5 extended structure for Ala. The conformational results obtained in this part are similar to those obtained in literature [27,39,44,45,46].

(B) = Ac-*Cage-Cage-NHMe*. One of the main conclusions reached in the case of [A] was that the MD simulation temperature of 300 K was adequate for complete exploration of peptides containing natural amino acids [27,39,44,45,46]. However, in the case of the highly strained PCU cage peptide, initial investigations (Figure 7[B]) revealed that 300 K was insufficient for the satisfactory exploration of the conformational space of this peptide sequence as the MD result did not correspond to the SA result as was the case with the non-cage sequences. In addition, with a different starting structure the PCU cage peptide is also trapped in a local minimum energy region, as can be observed when Figure 7[B] is compared with Figure 7[B']. Both these results were obtained at 300 K.

In order to compare the conformational explorations of MD simulations at different temperatures, higher temperatures ranging from 500 K to 900 K were explored. A summary of the conformational search for [B] using the elevated temperature MD simulations from 400 K through to 900 K, is shown in the Ramachandran plots depicted in Figure 8. The results presented in Figure 8, at 600 K, show nicely how MD is able to overcome rotational energy barriers between the different conformations. Indeed, the results obtained at 900 K are similar to the corresponding Ramachandran plots in Figure 5[B] obtained using SA. It is clear that 600 K is probably the lowest temperature required to overcome rotational barriers in a system containing the cage amino acid. Clearly, the replacement of Ala in the (i) and (i+1) positions with the PCU cage peptide results in a more restricted conformational space at 300 K. These plots are slightly different from the less restricted conformational space shown by the corresponding Ramachandran plot for SA in Figure 5[B]. This means that for MD, the clustering of backbone torsion angles is associated with only the α-helical structures, in contrast to C_{7ax} and C_{7eq} conformers observed in the case of SA calculations.

(C) = Ac-*Ala-Cage-NHMe*. The results of the conformational profile at various temperatures obtained in [B] = Ac-cage-cage-NHMe above suggests that 900 K closely resembled the conformational space explored in Figure 5[B] using SA. In contrast to the results obtained for the Ramachandran plots shown in Figure 5[C], the conformational space at 300 K is now quite restricted. Thus, the MD simulation for this peptide sequence was also carried out at both 300 K (Figure 7[C]) and at 900 K (Figure 9[C]). In the case of Ala in the (i) position, only the first and second quadrants are populated, which characterizes the C_5 extended structure of Ala. This is evident at 300 K and at 900 K. On the other hand, with the PCU cage residue in the (i+1) position, at 300 K the conformational space is restricted to only the first and third quadrants, whereas a greater flexibility of the backbone torsion angles is observed at 900 K, similar to [B] = Ac-cage-cage-NHMe. From the Ramachandran plots for 900 K in Figure 9[C] and the SA result in Figure 5[B], it is clear that the presence of Ala in the (i) position results in a greater conformational flexibility for the PCU cage residue in the (i+1) position. Also with the PCU cage in the (i) position for sequence [B], the conformational space of the PCU cage in the (i+1) position is restricted by steric hindrance. This result is indicative of the fact that the PCU cage residue in the (i+1) has a tendency to maintain the α-helical structure as well as the hydrogen-bonded C_{7ax} structures as illustrated by the Ramachandran plots in Figure 5[B] and Figure 9[C]. However, the low-energy conformers show clustering around torsion angles associated with C_5 extended structures, which is the expected result for

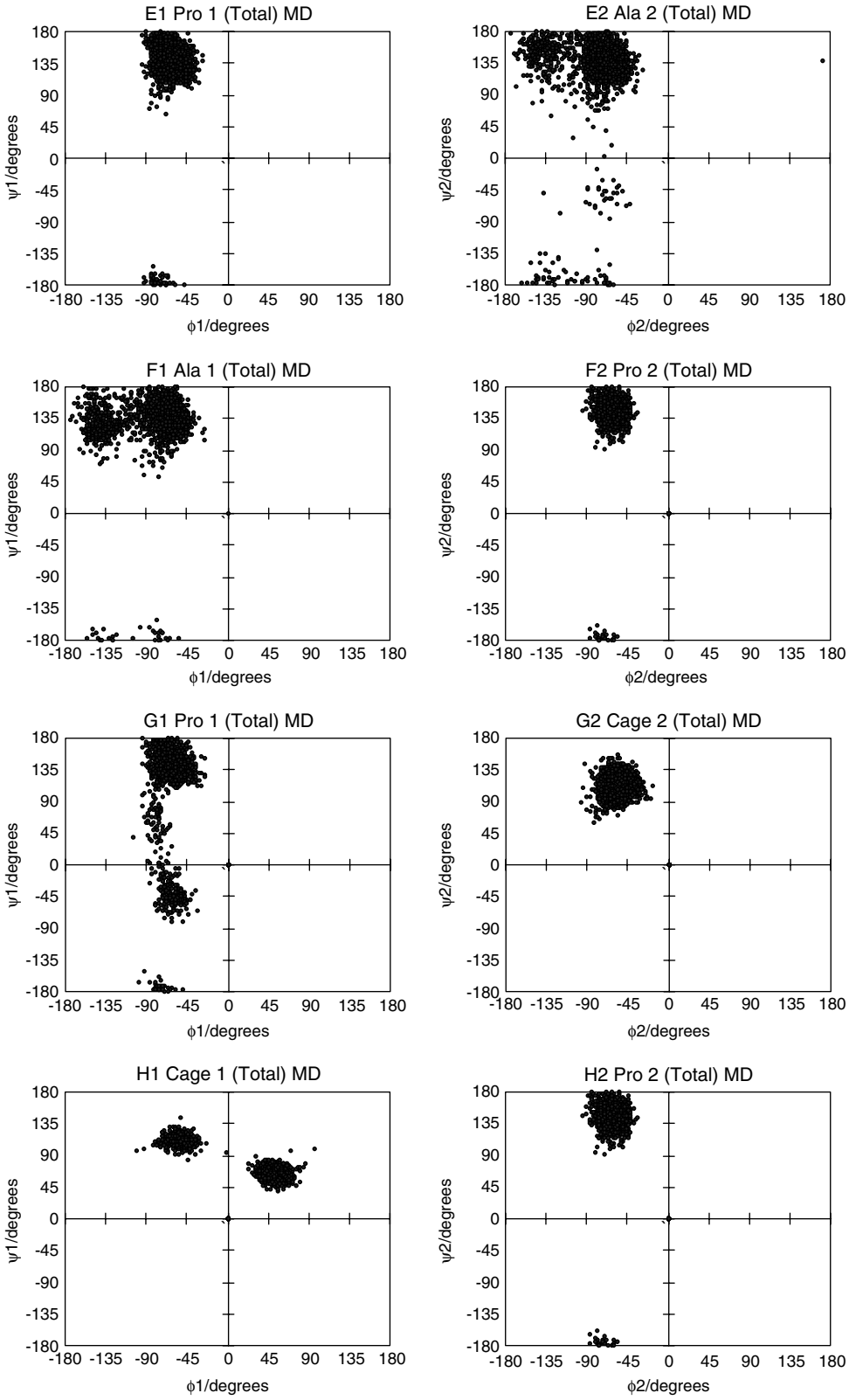

Figure 7[E]–[H] Ramachandran MD plots obtained at 300 K for the peptide sequences [E]–[H].

Ala [32], while the PCU cage residue in the second position is characterized by C_{7ax} structures, similar to the corresponding SA results displayed in Figure 5[C].

(D) = Ac-*Cage-Ala-NHMe*. The result of the conformational search using MD simulations, shown in Figure 7[D], reveals that at 300 K, the PCU cage residue

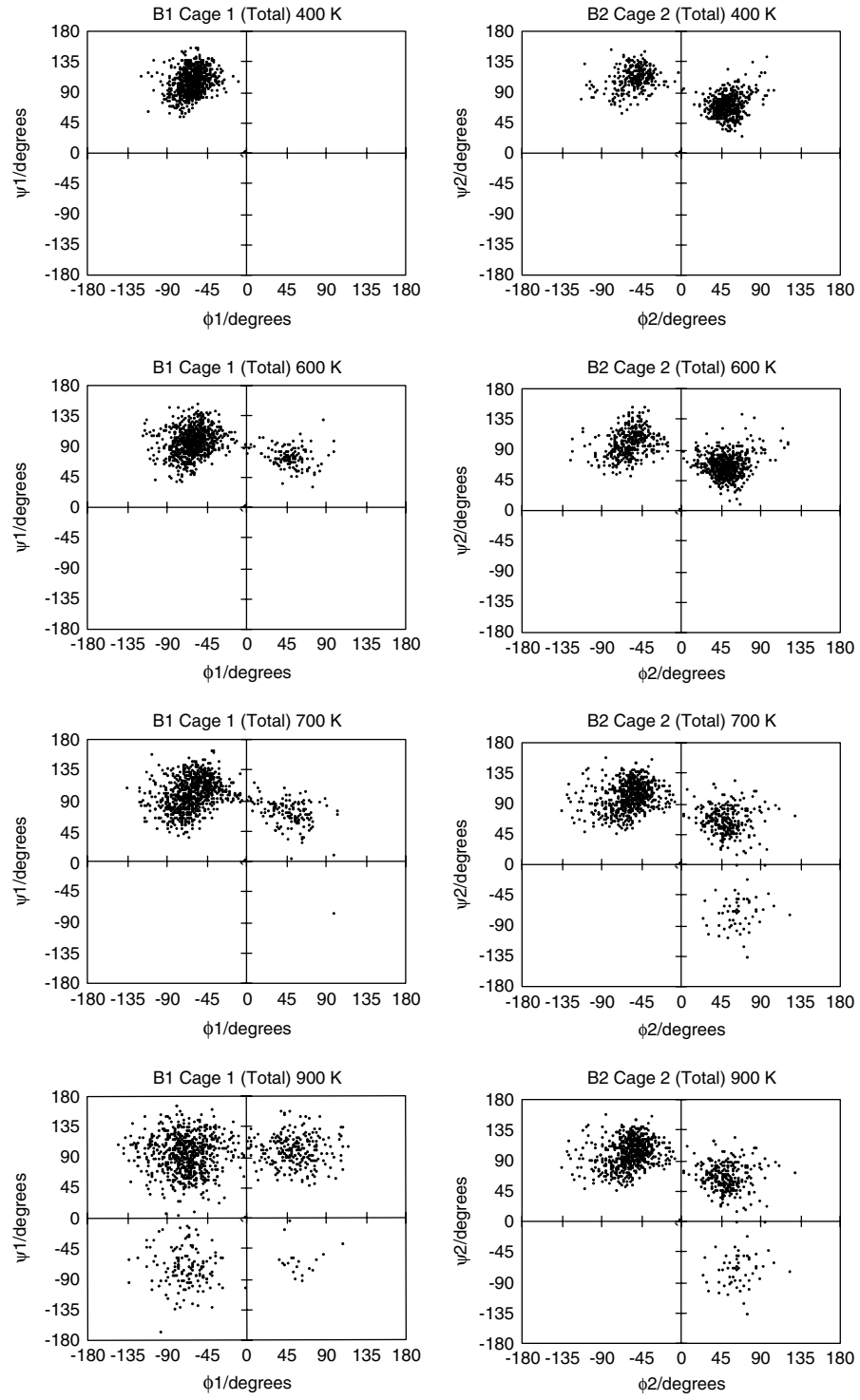

Figure 8[B] Temperature profile of the Ramachandran MD plots obtained for [B] = Ac-cage-cage-NHMe.

is trapped in the global minimum energy region. In this case, only the first quadrant is explored, in contrast to the first and third quadrants explored by the corresponding cage residue shown in Figure 9[C] at 900 K. A greater flexibility of the backbone torsion angles is observed at 900 K (Figure 9[D]), similar to the peptide sequences [B] = Ac-cage-cage-NHMe and [C] = Ac-Ala-cage-NHMe described above.

(E) = Ac-*Pro-Ala-NHMe*. The result of the conformational search using MD simulations at 300 K is shown in the Ramachandran plot depicted in Figure 7[E]. These results fit expectations since the conformational profile closely resembles that of Pro and Ala in the (i) and (i+1) positions respectively. In both cases, the low-energy conformers correspond to relatively extended conformations, similar to the result obtained

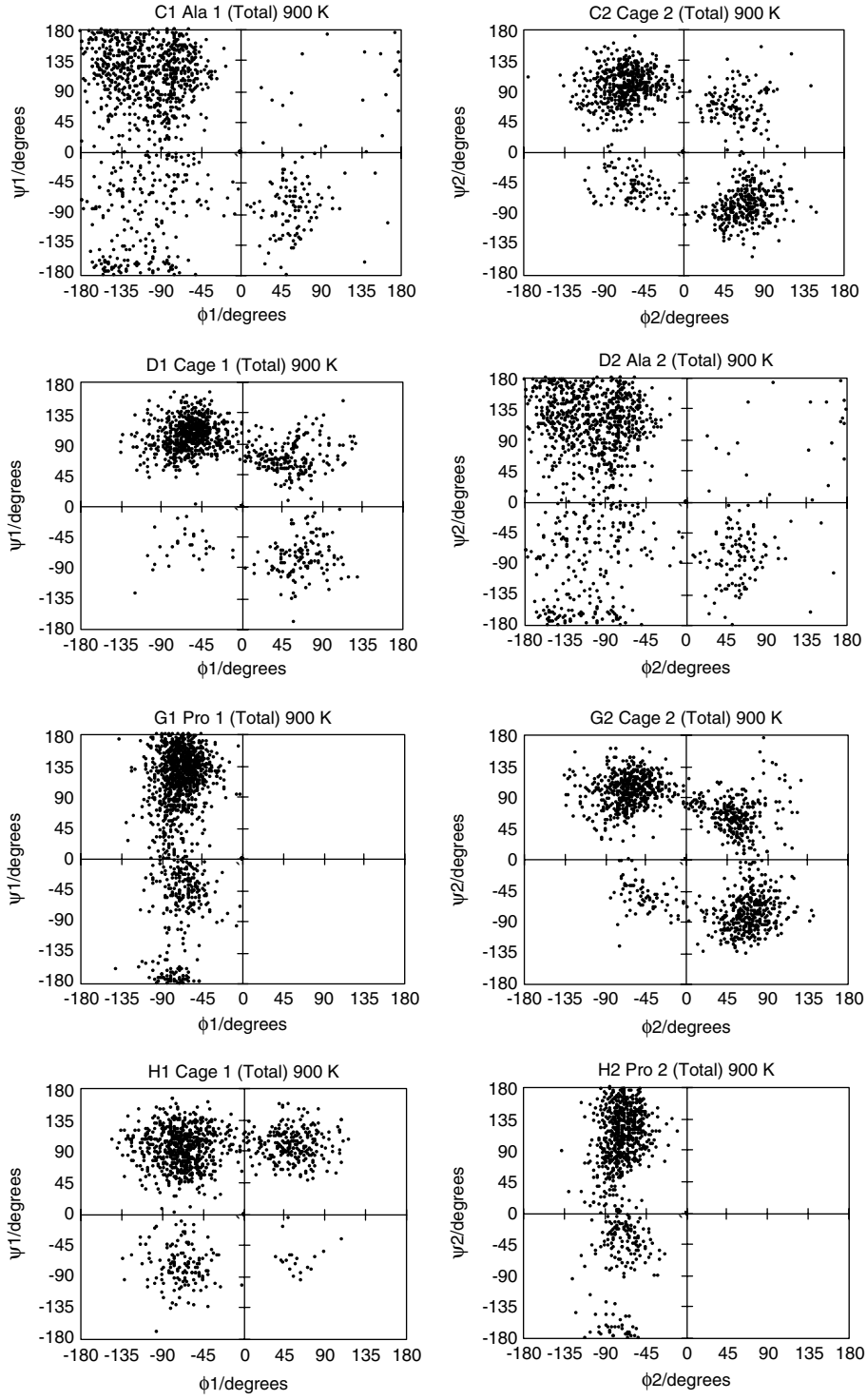

Figure 9 Temperature profile of the Ramachandran MD plots obtained for the peptide sequences [C], [D], [G] and [H] at 900 K.

in Figure 5[D] using SA. This demonstrates that 300 K was sufficient for the MD trajectory of Ala, and the results are consistent with those obtained by Chalmers and Marshall [32].

(F) = Ac-*Ala-Pro-NHMe*. The MD conformational results at 300 K in Figure 7[F] closely resembles the corresponding SA results shown in Figure 5[F]. This means that the same conformational space is explored using both SA and MD techniques. This result is consistent with those observed in literature [32–34].

(G) = Ac-*Pro-Cage-NHMe*. The exploration of the conformational space of this peptide sequence was carried out at 300 K and 900 K. The Ramachandran plots are shown in Figures 7[G] and 9[G] respectively.

At 300 K the replacement of Ala with the PCU cage residue in the (i+1) position results in the conformation being trapped in a local minimum, whereas at 900 K a greater conformational flexibility is observed. In the case of Pro at 300 K, the conformational space is limited to the first quadrant only, which is similar to the Ramachandran plots obtained with SA shown in Figure 5[G]. This is attributed to the steric interaction between the bulky Pro ring and the bulky cage structure on the C^{α} atom of the PCU cage residue. In this quadrant, the backbone torsion angles are characteristic of the C_{7ax} ring structure. The significance of this result is that in the case of the PCU cage residue being in the (i+1) position, the α-helical conformations observed in the non-Pro sequences are absent.

(H) = Ac-*Cage-Pro-NHMe*. The MD conformational study was carried out at 300 K and 900 K. The conformational profiles shown in Figures 9[G] and 9[H], are similar except that the PCU cage residue in the (i+1) position (Figure 7[G]) is trapped in a local minimum energy region at 300 K. The result serves as confirmation of the fact that 300 K is not sufficient for the complete exploration in cases involving the PCU cage peptide. The overall conformational profile of this peptide sequence is similar to the corresponding results obtained in Figures 5[G] and 5[H] for SA.

CONCLUSIONS

The two alternative computational methods, SA and MD provided a good sampling of the low-energy conformations of the molecules studied. Although the conformations found by the two methods are not identical, the overall conformational space of the peptides obtained using the two methods is in reasonable agreement. Conformations that have not been found by one or the other of the sampling procedures are however observed at higher energy values. This observation supports the hypothesis that the two procedures are capable of providing a complete sampling of the lowest energy conformational space of a peptide, and consequently, the results obtained by the two methods are self-consistent. Comparison of the results obtained in the present work using the two different computational methods suggests that the iterative SA procedure samples more quickly the different low-energy conformers with the lowest sampled energy minimum, located in different valleys of the peptide landscape.

One of the most significant observations with respect to the PCU cage peptide and MD simulations is that 300 K was insufficient to overcome the high rotational energy barriers posed by the rigid cage skeleton. The results from this study revealed that MD temperatures of $\geq$600 K were required for the complete exploration of the conformational landscape of the peptide analogues containing the PCU cage residues.

The results of the Ramachandran plots reveal that Pro has a tightly restricted conformational space in comparison with Ala and the PCU cage residues. Nevertheless this study also revealed that the inclusion of Ala, Pro and the PCU cage residues in the peptide sequences, [A]–[H], promote the stabilization of reverse-turn characteristics. Moreover the results suggest that the residues can also be accommodated in the (i) and (i+1) positions, resulting in β-turns. Indeed both techniques reveal that the presence of the very bulky cage-like structure on the C^{α} of the PCU cage residue imposes a marked restriction on the available conformational space. The cage in position (i) enhances the β-turn of the non-natural peptide.

Acknowledgements

K. B. gratefully acknowledges the support of the 'Centre de Supercomputació de Catalunya' (CESCA) for the generous allocation of computer time. The advice from Professors E. Giralt and T. A. Ford is gratefully acknowledged. Financial support for this research was made possible by the University of KwaZulu-Natal, Durban, the National Research Foundation Gun 2 046 819 (South Africa), the Ernest Oppenheimer Memorial Trust, and Durban Institute of Technology.

REFERENCES

1. Brookes KB, Hickmott PW, Jutle KK, Schreyer CA. Introduction of pharmacophoric groups into polycyclic systems. Part 4. Aziridine, oxiran and tertiary beta-hydroxyethylamine derivatives of adamantane. *S. Afr. J. Chem.* 1992; **45**: 8–11.
2. Davies WL, Hoffmann EC, Paulshock M, Wood TR, Haff RF, Grunert RR, Watts JC, Hermann EC, Neumayer EM, McGahen JW. Antiviral activity of 1-adamantane (Amantadine). *Science* 1964; **144**(362): 862–863.
3. Marchand AP. Synthesis and chemistry of homocubanes, biscubanes and trishomocubanes. *Chem. Rev.* 1989; **89**: 1011–1033.
4. Griffin GW, Marchand AP. Synthesis and chemistry of cubanes. *Chem. Rev.* 1989; **89**: 997–1010.
5. Marchand AP. In *Advances in Theoretically Interesting Molecules*, vol. 1, Thummel RP (ed.). JAI Press: Greenwich, 1989; 357–399.
6. Ranganathan D, Haridas V, Madhusudanan KP, Roy R, Nagaraj R, John GB, Sukhaswami MB. Design, synthesis and ion-transport properties of a novel family of cyclic adamantane-containing cystine peptides. *Angew. Chem. Int. Ed. Engl.* 1996; **35**: 1105–1107.
7. Aigami K, Inamoto Y, Takaishi N, Fujikura YJ, Takatsuki A, Tamura G. Biologically-active polycycloalcanes. Part 2. Antiviral 4-homoisotwistane derivatives. *J. Med. Chem.* 1976; **19**(4): 536–450.
8. Inamoto Y, Aiyami K, Kadono T, Nakayama H, Takatsuki A, Tumura G. Biologically-active polycycloalkanes. Part 4. Phosphoric ester of trimethylenenorbornyl alcohols. *J. Med. Chem.* 1977; **20**(11): 1371–1374.
9. Boeyens JCA, Cook LM, Nelson GN, Fourie TG. Conformation and drug activity of pentacyclo-undecanes. *S. Afr. J. Chem.* 1994; **47**(2): 72–75.
10. Geldenhuys WJ, Malan SF, Bloomquist JR, Marchand AP, Van der Schyf CJ. Pharmacology and structure-activity relationships

of bioactive polycyclic cage compounds: a focus on pentacycloundecane derivatives. *Med. Res. Rev.* 2005; **25**(1): 21–48.
11. Oliver DW, Dekker DG, Snykers FO. Pentacyclo[5.4.0.0^{2,6}.0^{3,10}.0^{5,9}] undeccylamine – synthesis and pharmacology. *Eur. J. Med. Chem.* 1991; **26**(4): 375–379.
12. Oliver DW, Dekker DG, Snykers FO. Antiviral properties of 4-amino-(D3)-trishomocubanes. *Drug. Res.* 1991; **41–1**(5): 549–552.
13. Oliver DW, Dekker DG, Snykers FO. Synthesis and biological activity of D3-trishomocubyl-4-amines. *J. Med. Chem.* 1991; **34**(2): 851–854.
14. Noren CJ, Anthoney-Cahill SJ, Griffith MC, Schultz PG. A general method for site-specific incorporation of unnatural amino-acids into proteins. *Science* 1989; **244**(4901): 182–188.
15. Roesser JR, Chorghade MS, Hecht SM. Ribosomecatalyzed formation of an abnormal peptide analogue. *Biochemistry* 1986; **25**: 6361–6365.
16. Hanessian S, McNaughton-Smith G, Lombart HG, Lubell WD. Design and synthesis of conformationally constrained amino acids as versatile scaffolds and peptide memetics. *Tetrahedron* 1997; **53**(38): 12 789–12 854.
17. Gerzon K, Kou D. Adamantyl group in medicinal agents. Part 3. Nucleoside 5-adamantoates. Adamantoyl function as protecting group. *J. Med. Chem.* 1967; **10**(2): 189–199.
18. Rapala RT, Kraay RJ, Gerzon K. Adamantyl group in medicinal agents. Part 2. Anabolic steriod 17 beta-adamantoates. *J. Med. Chem.* 1965; **8**: 580–583.
19. Voldeng AN, Bradley CA, Kee RD, King EL, Melder FL. Synthesis of adamantyl analogues of analgesics. *J. Pharm. Sci.* 1968; **57**: 1053–1055.
20. Martins FJC, Viljoen AM, Kruger HG, Fourie L, Roscher J, Joubert JA, Wessels PL. Enantioselective synthesis of amino acids from pentacyclo[5.4.0.0^{2,6}.0^{3,10}.0^{5,9}]undecane-8,11-dione. *Tetrahedron* 2001; **57**: 1601–1607.
21. Bisetty K, Gomez-Catalan J, Aleman C, Giralt E, Kruger HG, Perez JJ. Computational study of the conformational preferences of the (R)-8-amino-pentacyclo[5.4.0.0^{2,6}.0^{3,10}.0^{5,9}] undecane-8-carboxylic acid monopeptide. *J. Pept. Sci.* 2004; **10**: 274–284.
22. Gould IR, Cornell WD, Hillier IH. A quantum-mechanical investigation of the conformational energetics of the alanine and glycine dipeptides in the gas-phase and in aqueous solution. *J. Am. Chem. Soc.* 1994; **116**(20): 9250–9256.
23. Cornell WD, Gould IR, Kollman PA. The effects of basis set and blocking groups on the conformational energies of glycyl and alanyl dipeptides. *J. Mol. Struct. (Theochem.)* 1997; **392**: 101–109.
24. Kirkpatrick S, Gelatt CD, Vecchi MP. Optimization by simulated annealing. *Science* 1983; **220**(4598): 671–680.
25. Filizola M, CarteniFarina M, Perez JJ. Conformational study of vasoactive intestinal peptide by computational methods. *J. Pept. Res.* 1997; **50**(1): 55–64.
26. Centeno NB, Perez JJ. A proposed bioactive conformation of peptide T. *J. Comput. Aided Mol. Des.* 1998; **12**(1): 7–14.
27. Shobana S, Vishveshwara S. Conformational study of valinomycin: a molecular dynamics approach. *Biophys. Chem.* 1996; **57**(2–3): 163–175.
28. Corcho FJ, Filizola M, Perez JJ. Assessment of the bioactive conformation of the farnesyltransferase protein binding recognition motif by computational methods. *J. Biomol. Struct. Dyn.* 1999; **16**(5): 1043–1052.
29. Leach AR. *Molecular Modelling: Principles and Applications*. Addison Wesley Longman: 1996; 413–436.
30. Lybrand TP. In computer simulation of biomolecular systems using molecular dynamics and free energy perturbation methods. In *Reviews in Computational Chemistry*, vol. 1, Lipkowitz KB, Boyd DB (eds.) VCH Publishers: New York, 1990; 295–320.
31. Brooks CL III, Karplus M, Pettitt BM. In proteins: a theoretical perspective of dynamics, structure, and thermodynamics. In *Advances in Chemical Physics*, vol. LXXI, Prigonine I, Rice SA (eds.) John Wiley & Sons: New York, 1985; 35–44.
32. Chalmers DK, Marshall GR. Pro-D-amino acid and D-Pro-NHMe-amino acid – simple, efficient reverse-turn constraints. *J. Am. Chem. Soc.* 1995; **117**(22): 5927–5937.
33. Möhle K, Gubmann M, Hofmann H-J. Structural and energetic relations between beta turns. *J. Comput. Chem.* 1997; **18**(11): 1415–1430.
34. Rose GD, Gierasch LM, Smith JA. Turns in peptides and proteins. *Adv. Protein Chem.* 1985; **37**: 1–109.
35. Case DA, Pearlman DA, Caldwell JW, Cheatham III TE, Ross WS, Simmerling CL, Darden TA, Merz KM, Stanton RV, Cheng AL, Vincent JJ, Crowley M, Ferguson DM, Radmer RJ, Seibel GL, Singh UC, Weiner PK, Kollman PA. *AMBER 5.0*. University of California: San Francisco, 1997.
36. Jorgensen WL, Chandrasekhar J, Madura JD, Imprey RW, Klein ML. Comparison of simple potential functions for simulating liquid water. *J. Chem. Phys.* 1983; **79**(2): 926–935.
37. York DM, Darden TA, Pedersen LG. The effect of long-range electrostatic interactions in simulations of macromolecules – a comparison of the Ewald and truncated list methods. *J. Chem. Phys.* 1993; **99**(10): 8345–8348.
38. Endrédi G, Perczel A, Farkas O, McAllister MA, Csonka GI, Ladik J, Csizmadia IG. Peptide models. Part 15. The effect of basis set size increase and electron correlation on selected minima of the *ab initio* 2D-Ramachandran map For-Gly-NH_2 and For-L-Ala-NH_2. *J. Mol. Struct. (Theochem.)* 1997; **391**(1–2): 15–26.
39. Venkatachalam CM. Stereochemical criteria for polypeptides and proteins. Part 5. Conformation of a system of 3 linked peptide units. *Biopolymers* 1968; **6**(10): 1425–1436.
40. Höltje HD, Folkers G. *In Methods and Principles in Medicinal Chemistry*, vol. 5. VCH Publishers: New York, 1996; 81–88.
41. Gomez-Catalan J, Perez JJ, Jimenez AI, Cativiela C. Study of the conformational profile of selected unnatural amino acid residues derived from L-phenylalanine. *J. Pept. Res.* 1999; **5**: 251–262.
42. De la Figuera N, Alkorta I, García-López MT, Herranz R, González-Muñiz R. 2-Amino-3-oxohexahydroindolizino[8,7-B]indole-5-carboxylate derivatives as new scaffolds for mimicking beta-turn secondary structures – molecular dynamics and stereoselective synthesis. *Tetrahedron* 1995; **51**(28): 7841–7856.
43. Rao SN, Ramnarayan K, Chan MF, Balaji VN. Conformations of model peptides with 1-aminocycloalkane-1-carboxylic acid residues. *Protein Pept. Lett.* 1996; **3**(1): 31–38.
44. Böhm HJ, Klebe G, Lorenz T, Mietzner T, Siggel L. Different approaches to conformational-analysis – a comparison of completeness, efficiency and reliability based on the study of a 9-membered lactam. *J. Comput. Chem.* 1990; **11**(9): 1021–1028.
45. Filizola M, Centeno NB, Farina MC, Perez JJ. Conformational analysis of the highly potent bradykinin antagonist Hoe-140 by means of two different computational methods. *J. Biomol. Struct. Dyn.* 1998; **15**(4): 639–652.
46. Canto CR, Schimmel PR. *Biophysical Chemistry. Part 1: The Conformation of Biological Molecules*. W.H. Freeman: New York, 1980; 253–281.